An Adaptive Time-Stepping Algorithm in Weakly Coupled Electromagnetics-Thermal-Circuit Modeling

R. B. B. Ovando-Martinez, C. Hernandez, and M. A. Arjona

División de Estudios de Posgrado e Investigación
Instituto Tecnológico de La Laguna, Torreón, Coah. 27000, Mexico
ronat-13@hotmail.com, coni.hernandez@ieee.org, and marjona@ieee.org

Abstract **─** This paper presents a weakly coupled formulation for the electromagnetic and thermal fields by applying the backward differentiation formula (BDF) and the Theta algorithm for the adaptive time-stepping and variable order 2D finite-element discretization. A coupling of the electromagnetic diffusion equation (EDE) and the electrical circuit equations is also included. A minimum time step criterion is adopted and an algorithm for the time-step size and order selection is implemented. The proposed model was programmed in C language. An example is presented to show the application of the formulation.

Index Terms - Coupling, electrical circuits, electro-thermal analysis, finite elements, and time-stepping.

I. INTRODUCTION

The coupled problem analysis (CPA) involves the coupling and solution of two or more partial differential equations (PDE's) [1]. Recently, the CPA has been applied in electromagnetics, thermal and fluid flow field problems for solving power quality troubles in electrical and electronic devices [2-5]. The use of modern numerical techniques and advanced computational tools makes possible the CPA. The finite element is a numerical technique used for solving space and time domain PDE's [6, 7]. A huge amount of numerical processes take place in a transient CPA computation. Fast and efficient algorithms are required for the transient CPA. Numerical methods based on constant time steps, such as the Euler methods, are not appropriate in a transient CPA due to the high computational time that is required [8]. Instead, variable time-stepping strategies are recommended [9]. The backward differentiation formula (BDF) is a variable time-stepping method, which is A-stable and L-stable and is recommended for solving stiff problems [10, 11]. The Theta algorithm is a non-variable time-stepping method, where the parameter θ is chosen such that $0 \leq \theta \leq 1$ and different solution schemes are obtained [12, 13]. A finite element (FE) BDF-Theta strategy has been successfully implemented for solving the transient EDE [14].

In this paper, the BDF-Theta strategy reported in [14] is applied for solving a weakly coupled electro-thermal 2D-FE transient formulation. The methodology is applied using 2D first-order triangular elements. A coupling of the EDE and the electrical circuit equations is included in the model [15]. A suitable minimum FE time-step criterion is adopted to avoid small time steps and instability. An algorithm for the proper time-step and order selection is implemented. An error control criterion and an initial guess prediction algorithm are applied for convergence acceleration. The developed formulation was applied to compute the magnetic vector potential, temperature distributions, and induced electrical current in a metallic slab close to a conductor fed with a voltage source. The model formulation was programmed in C language.

II. DOMAIN EQUATIONS

A CPA is carried out for the electro-thermal analysis of an electrical device. An electro-thermal analysis is commonly required in the design of electrical motors, generators, and transformers

Submitted On: Dec. 13, 2012
Accepted On: Aug. 29, 2013

1054-4887

[16-18]. This paper develops an electro-thermal CPA model. Therefore, the EDE and the heat equation (HE) are the subject of this paper. The EDE and the HE are described by a diffusion type PDE as in equation (1),

$$C_1 \nabla^2 f = -S_o + C_2 \frac{\partial f}{\partial t} \tag{1}$$

where f is a function, $C_{1,2}$ are constants, S_o is a source function, and t the time. The EDE and the HE are properly obtained considering the list of symbols shown in Table I. However, in electric devices modeling some special considerations in the EDE must be considered. The electric devices may be fed by voltage sources and/or current sources (see Table I) and they present a variety of electrical connections.

Equations (2) and (3) show the formulation of the EDE for thick conductors that are fed by a voltage source [14],

$$\frac{1}{\mu}\nabla^2 A = -\sigma\frac{V}{\ell} + \sigma\frac{\partial A}{\partial t} \tag{2}$$

$$V = RI + R\int_{S_t} \sigma \frac{\partial A}{\partial t}\, dS_t \,, \tag{3}$$

where V is the voltage, R represents the resistance, I the current, σ the electrical conductivity, ℓ the length, and S_t the total surface of the conductor. The resistance R for thick conductors is defined as,

$$R = \frac{\ell}{\sigma S_t}\,. \tag{4}$$

Table I: Equivalent symbols for the EDE and HE.

	f	*S_o*	*C_1*	*C_2*
EDE	*Magnetic Potential*	*Current density*	*Reluctivity*	*Electric Conductivity*
	A (Wb/m)	*J and/or σV/ℓ (A/m²)*	*υ (m/H)*	*σ (S/m)*
HE	*Temperature*	*Power density*	*Thermal Conductivity*	*Mass density product Specific heat*
	T (°K)	*q (W/m³)*	*k (W/(m°K))*	*P ·C_p (kg/m3, J/(kg°K))*

The power loss density is calculated with equations (2) and (3). Afterwards, the HE is used to obtain the temperature distribution.

III. FINITE ELEMENT MODEL

The set of equations (1)-(4) is solved using first order triangular FE and the Galerkin residuals. Equations (5) and (6) show the FE discretization for the EDE, HE, and the electric circuit equations,

$$C_2\left[T_{ij}\right]\left\{\frac{\partial f_j}{\partial t}\right\} = C_1\left[M_{ij}\right]\left\{f_j\right\} + S_o\left\{G_i\right\} \tag{5}$$

$$V = RI + \sum_m\left(\frac{R\sigma S}{3}\sum_{g=1}^{3}\left(\frac{A_g^{n+1} - A_g^n}{\Delta t}\right)\right), \tag{6}$$

where,

$$\left[T_{ij}\right] = \int_\Omega N_i N_j d\Omega\,, \tag{7}$$

$$\left[M_{ij}\right] = -\int_\Omega\left(\frac{\partial N_i}{\partial x}\frac{\partial N_j}{\partial x} + \frac{\partial N_i}{\partial y}\frac{\partial N_j}{\partial y}\right)d\Omega\,, \tag{8}$$

$$\left\{G_i\right\} = \int_\Omega N_i d\Omega\,, \tag{9}$$

where i and j stand for the nodes numbers, n is the time step number, Δt is the time-step defined as $\Delta t = t_{n+1} - t_n$, $N_{i,j}$ represents the 2D first-order triangular FE shape functions, m is the number of elements conforming a conductor, S is the area of the triangular element, and g is the local node numbering in a triangular element. By introducing a parameter θ in equation (5) such that,

$$f_j^{n+\theta} = \theta f_j^{n+1} + (1-\theta) f_j^n \tag{10}$$

$$G_i^{n+\theta} = \theta G_i^{n+1} + (1-\theta) G_i^n\,, \tag{11}$$

the theta scheme in equation (12) is obtained as follows,

$$C_2\left[T_{ij}\right]\left\{\frac{\partial f_j^{n+\theta}}{\partial t}\right\} = C_1\left[M_{ij}\right]\left\{f_j^{n+\theta}\right\} + S_o\left\{G_i^{n+\theta}\right\}. \tag{12}$$

The Taylor series are used to obtain a linear approximation of the temporal partial differentiation in equation (12) as,

$$\frac{\partial f_j^{n+\theta}}{\partial t} = \frac{f_j^{n+1} - f_j^n}{\Delta t}\,. \tag{13}$$

Nevertheless, the resulting equation gives stable results for $\theta > 1/2$ as the time step $\Delta t \rightarrow 0$ [12]. The Taylor series approximation in equation (13) involves fixed time steps that lead to large computation times. An alternative approximation for the temporal partial differentiation in equation (12) is the implementation of the BDF. The BDF is a variable time-stepping algorithm that allows savings in the computational time. In addition, the BDF has good stability properties for orders less than sixth [10].

In the next section the BDF-Theta algorithm developed in [14] has been implemented to solve the weakly coupled electro-thermal problem described by equation (12).

IV. BDF-THETA ALGORITHM

The BDF-Theta includes the damping characteristics of the theta algorithm and the variable time-stepping and order algorithms of the BDF method. The effectiveness and accuracy of the BDF-Theta method is reported in [14] where the model results have been compared against an analytical solution. The arithmetic operations performed with the BDF-Theta are smaller in comparison with the Runge-Kutta methodologies [8, 14, 19-20]. Different schemes of solution depending on θ are obtained from the BDF-Theta method, e.g., the implicit scheme of the BDF-Theta method leads to the common BDF-implicit solver strategies, such as the ones used in the DASSL code [10]. The implementation of the BDF-Theta produces a nonlinear system of equations that are solved by the Newton-Raphson (NR).

Once the BDF-Theta algorithm is applied in equation (12), the residual and Jacobian are obtained by equations (14) and (15), respectively,

$$\{R_i\} = C_1[M_{ij}]\{f_j^{n+\theta}\} + S_o\{G_i^{n+\theta}\} + C_2[T_{ij}]\left\{\frac{1}{\Delta t}\sum_{g=0}^{K} f_j^{n+1-g}\alpha_g\right\} \quad (14)$$

$$[Jac_{i\beta}] = \theta C_1[M_{i\beta}] + C_2[T_{i\beta}]\left\{\frac{\alpha_0}{\Delta t}\right\}, \quad (15)$$

where K represents the order and backward data required to evaluate equation (14).

The algebraic process to obtain α_g from equations (14) and (15) is described in [11] and it is defined as,

$$\alpha_g = \frac{(t_{n+1} - t_n)}{(t_{n+1} - t_{n+1-g})}\prod_{\substack{\psi=1 \\ \psi\neq g}}^{K}\frac{(t_{n+1} - t_{n+1-\psi})}{(t_{n+1-g} - t_{n+1-\psi})} \quad (16)$$

for $0 < g \leq K$, while for $g = 0$,

$$\alpha_0 = -\sum_{\psi=1}^{K}\alpha_\psi \,. \quad (17)$$

Equations (16) and (17) store information at t_{n+1-K}, which is used to evaluate the temporal partial differentiation in equation (12) at each time step. The solution of equations (14) and (15) is obtained by applying equation (18) and distinct schemes of solution are allowed by varying θ,

$$[Jac_{i\beta}]\{\Delta f_\beta^{n+1}\} = -\{R_i\} \quad (18)$$

where f^{n+1} are the unknown variables and f^n the last iteration values. The initial guess prediction algorithm can be implemented in equation (18) for the convergence acceleration [11, 21].

V. THE WEAKLY ELECTRO-THERMAL MODEL

The proposed weakly modeling is obtained from equations (14) and (15). The symbols in Table I are replaced into equations (14) and (15) to obtain the EDE and the HE. The residual and Jacobian for the EDE are shown in equations (19) and (20), respectively,

$$\{R_i^{EDE}\} = \upsilon[M_{ij}]\{A_j^{n+\theta}\} + \frac{\sigma U}{\ell}\{G_i^{n+\theta}\} + \sigma[T_{ij}]\left\{\frac{1}{\Delta t}\sum_{g=0}^{K} A_j^{n+1-g}\alpha_g\right\} \quad (19)$$

$$[Jac_{i\beta}^{EDE}] = \theta\upsilon[M_{i\beta}] + \sigma[T_{i\beta}]\left\{\frac{\alpha_0}{\Delta t}\right\}, \quad (20)$$

while the residual and the Jacobian for the HE are,

$$\{R_i^{HE}\} = k[M_{ij}]\{T_j^{n+\theta}\} + q\{G_i^{n+\theta}\} + \rho C_p[T_{ij}]\left\{\frac{1}{\Delta t}\sum_{g=0}^{K} T_j^{n+1-g}\alpha_g\right\}, \quad (21)$$

$$[Jac_{i\beta}^{HE}] = \theta k[M_{i\beta}] + \rho C_p[T_{i\beta}]\left\{\frac{\alpha_0}{\Delta t}\right\}. \quad (22)$$

The solution of equations (19) to (22) is obtained from equation (18). Equations (19) to (22) were programmed in C language and solved using a sparse direct solver [22-23]. The flowchart of the programmed code is shown in Fig. 1. In a first step, the meshing, the physical parameters, the simulation time t_s, and the boundary conditions are executed. The BDF-Theta proposes a minimum time-step constraint [14]. The use of a minimum time-step in the model avoids the presence of discontinuities in the numerical results and brings numerical stability [11, 14]. Reference [14] proposes a minimum time-step constraint Δt_{min} for the EDE as,

$$\Delta t_{EDE}^{\min} = C\cdot\mu\cdot\sigma\cdot h^2 \quad (23)$$

where C is a constant chosen such that $C \leq 1$ and h is related to the minimal FE size [13, 24]. However, in a CPA a minimum time-step per phenomenon must be defined. Wherefore, this paper proposes a minimum time-step constraint for the HE as,

$$\Delta t_{HE}^{\min} = C\cdot\rho\cdot C_p\cdot h^2\cdot\frac{1}{k}\,. \quad (24)$$

In a CPA model, the different time-step restrictions must be incorporated in an absolute minimum time-step Δt_{min}. This paper proposes the absolute minimum time-step strategy defined by equation (25),

$$\Delta t_{\min} = \frac{\Delta t_{EDE}^{\min} \Delta t_{HE}^{\min}}{\Delta t_{EDE}^{\min} + \Delta t_{HE}^{\min}}. \quad (25)$$

The time-step criterion in equation (25) has been successfully used for fluid flow analysis in [13]. Once the time-step defined in equation (25) is calculated, an initial guess prediction algorithm is performed for convergence acceleration as it is indicated in [14]. The convergence in equation (18) accelerates when the predicted values Ap^{n+1} and Tp^{n+1} are near to the system solution. Equations (19) and (20) are calculated until a certain relative error ε is accomplished. Afterwards, the coupled circuit equations at equation (6) are solved. The power loss density is calculated and used for solving equations (21) and (22). The power loss density is obtained as,

$$q = \sigma \left(\frac{\partial A}{\partial t} \right)^2 + \frac{J^2}{\sigma}. \quad (26)$$

The first term at the right hand side of equation (26) represents the power loss density due to the Eddy currents. The second term in equation (26) represents the power loss density due to the current or voltage sources (see Table I). Equation (26) is used in equations (21) to (22) and the HE is solved until a predefined relative error ε is achieved. The time loop is performed while $t_{n+1} \neq t_s$. A new order and a new time-step are calculated at each iteration. The Gear's algorithm has a suitable technique to calculate Δt and the K order at each time iteration [11]. The Gear's algorithm changes the K order up or down by defining a time step ratio η_K as,

$$\eta^j{}_K = \frac{\Delta t_{new}}{\Delta t} = \frac{\Delta f_j}{f_j^{n+1} - fp_j^{n+1}} \quad (27)$$

where $\eta^j{}_K$ is the time step ratio of the K order in the node jth, f refers to the unknown variables A and T at Table I, fp are the predicted values and Δf_j is an absolute error (error control) allowed in the jth unknown variable.

In this paper, the Δf_j quantities are the last iteration values from ΔA^{n+1} and ΔT^{n+1} in the NR. The maximum time-step ratio for the next iteration is chosen as $\eta_K = \min_{j \in NOD} \eta^j{}_K$ where NOD refers to the set of nodes in the FE mesh. The order K for the next iteration is obtained by comparing the quantities η_K, η_{K-1}, and η_{K+1} and selecting $\max_{K-1 \le Y \le K+1} \eta_Y$. The process to obtain the quantities η_K, η_{K-1}, and η_{K+1} is described in [11]. From the time loop, two different time steps (Δt_{EDE} and Δt_{HE}) and two orders (K_{EDE} and K_{HE}) are obtained. The order K_{EDE} is applied in equations (19) and (20) and the order K_{HE} is used in equations (21) and (22). An absolute time-step is obtained from Δt_{EDE} and Δt_{HE} using equation (25) as in equation (28),

$$\Delta t_{abs} = \frac{\Delta t_{EDE} \Delta t_{HE}}{\Delta t_{EDE} + \Delta t_{HE}}. \quad (28)$$

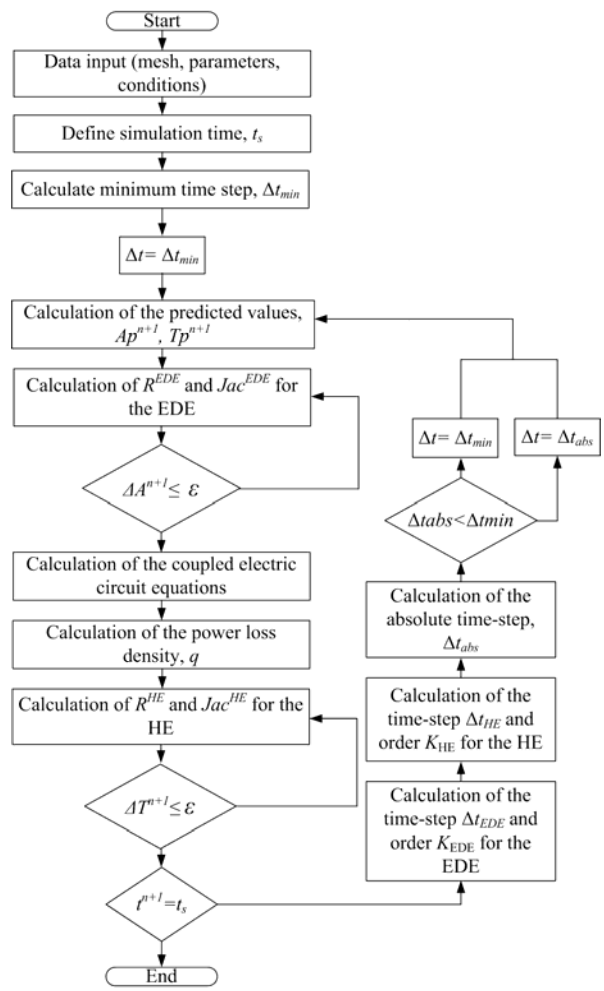

Fig. 1. Flowchart of the developed model.

Finally, the time-step Δt for the next iteration is selected as $\Delta t_{\min}$ if $\Delta t_{\text{abs}} \le \Delta t_{\min}$ and selected as Δt_{abs} if $\Delta t_{\min} \le \Delta t_{\text{abs}}$.

VI. NUMERICAL EXAMPLE

The problem domain and parameters for a nichrome wire placed above an aluminum slab are shown in Fig. 2. The nichrome wire is fed with a voltage source. The power loss density is generated by the electrical conductivity and the eddy currents. The power loss densities increment the temperature gradient in the domain. The Dirichlet boundary condition is used for the EDE and the HE.

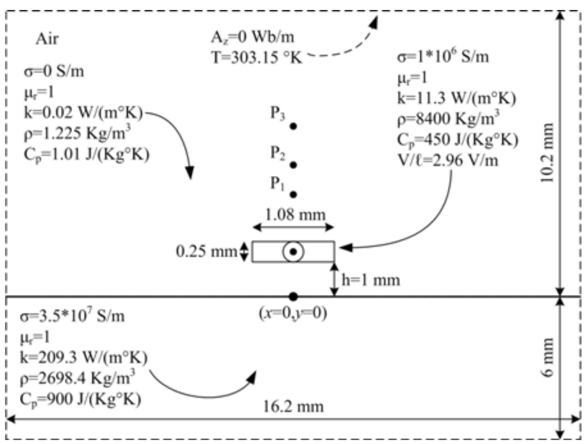

Fig. 2. Problem domain used in the numerical example.

The weakly electro-thermal CPA model shown in Fig. 1 was programmed in C language and solved for the domain illustrated in Fig. 2. The mesh has 2587 nodes and 5016 first order triangular elements. The model was executed in a laptop computer with a 2 GHz dual core processor and 2 GB RAM. Two numerical experiments were made for relative errors ε of 1E-1 and 1E-2 with θ=1. The modeling results are shown in Table II. It was found that for tighter relative errors ε the orders K_{EDE} and K_{HE} are higher and more stable as it is reported in Table II and shown in Figs. 3 and 4. It can be concluded that higher time-steps and lower time-loop iterations are attained for tighter relative errors in ε. The time-step Δt evolution throughout the simulation time is shown in Fig. 5.

It was found that the time-step is more stable for a tighter error ε. Nevertheless, the NR loop in the model causes a higher computation time for a tighter error ε. The proposed model was used to obtain the electromagnetic and thermal transient response at points P_1(0, 0.0019), P_2(0, 0.0023), and P_3(0, 0.003) shown in Fig. 2. The numerical results shown in Figs. 6 and 7 were obtained using an implicit scheme (θ=1) and a relative error of ε=1E-2. The transient solution for a simulated time of 150 *s* required 234 *s* of computation time. The steady state was attained after 1 m*s* of simulated time for the EDE and after 100 *s* for the HE. The time steps are short before the first 1 m*s* of simulated time due the small time constant of the EDE in equation (28). Afterwards, the time steps are larger due to the time constant of the HE in equation (28). The modeling results were compared against those obtained with a commercial software [25] and an error less than 1E-5 was achieved as it is shown in Figs. 6 and 7. The induced current density shown in Fig. 8 was estimated from the Eddy currents in the metallic slab and by solving the electric circuit equations given by equation (6). Finally, the potential distribution for the EDE and the HE are shown at Figs. 9 and 10. The electrical current in the nichrome wire at Fig. 2 produces the magnetic potential distribution shown in Fig. 9. The temperature distribution at Fig. 10 is caused by the Eddy currents in the metallic slab and by the power loss density obtained from the voltage source in the nichrome wire. The hot spot was located in the nichrome wire where the temperature rises 34 °K above the ambient temperature.

Table II: Numerical behavior obtained in the model for ε = 1E-1 and ε = 1E-2.

	ε=1*E*-1	**ε=1*E*-2**
Max K_{EDE}	5	5
Max K_{HE}	2	3
Max Δt	27.92	55.18
Time iterations	278	267
Computation time (s)	228	234

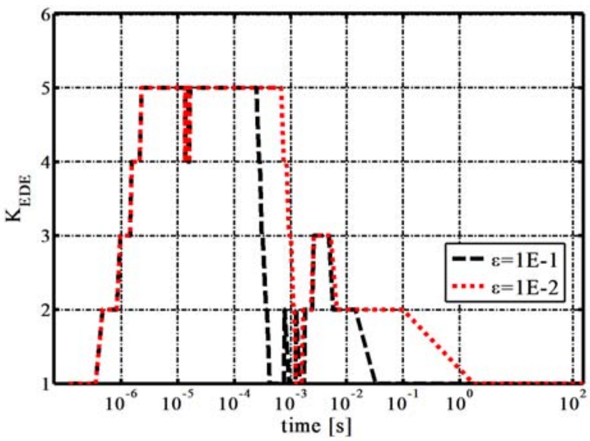

Fig. 3. Evolution of the order K_{EDE} for θ=1 and ε equals to 1E-1 and 1E-2.

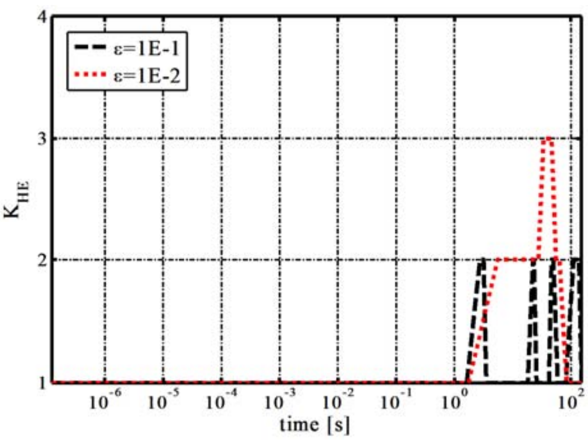

Fig. 4. Evolution of the order K_{HE} for θ=1 and ε equals to 1E-1 and 1E-2.

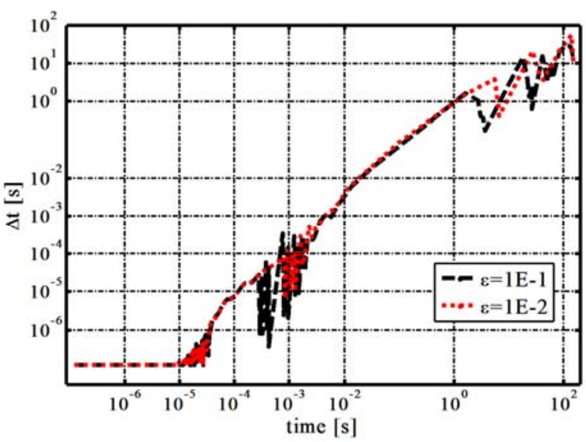

Fig. 5. Time-step Δt evolution for θ=1 and ε equals to 1E-1 and 1E-2.

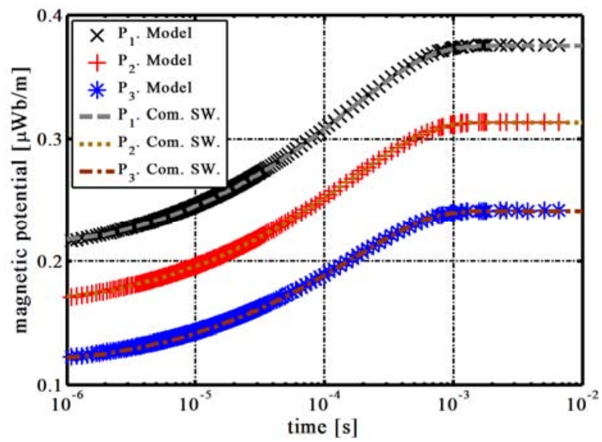

Fig. 6. Transient response of the EDE at points P_1, P_2, and P_3 for θ=1 and ε=1E-2. Results computed with the propose model (Model) and a commercial software (Com. SW.).

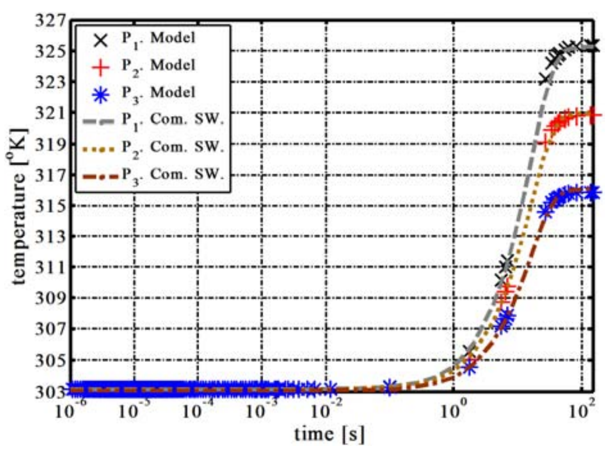

Fig. 7. Transient response of the HE at points P_1, P_2, and P_3 for θ=1 and ε=1E-2. Results computed with the propose model (Model) and a commercial software (Com. SW.).

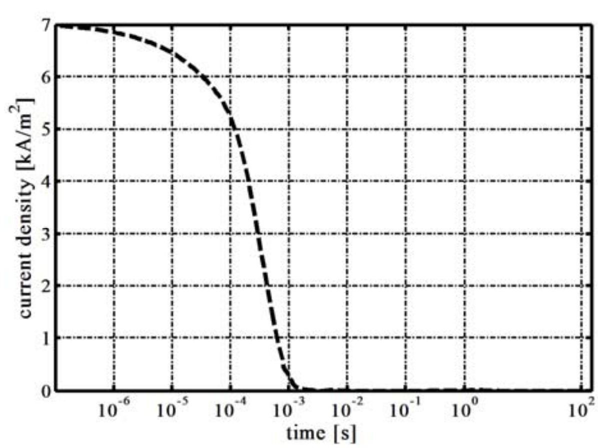

Fig. 8. Current density induced in the metallic slab.

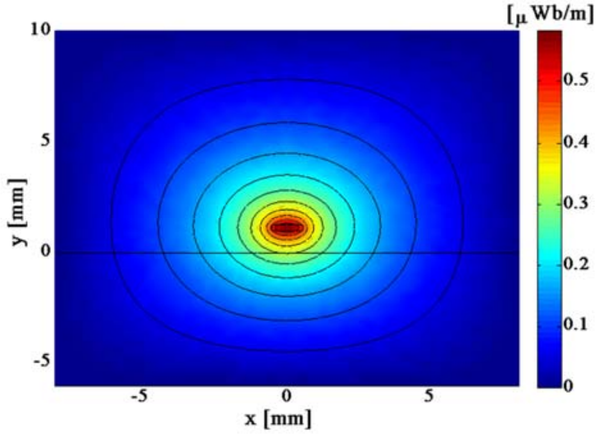

Fig. 9. Magnetic potential distribution computed at steady state for θ=1 and ε=1E-2. Max. Pot.: 5.82x10^{-7} Wb/m, Min. Pot.: 0 Wb/m.

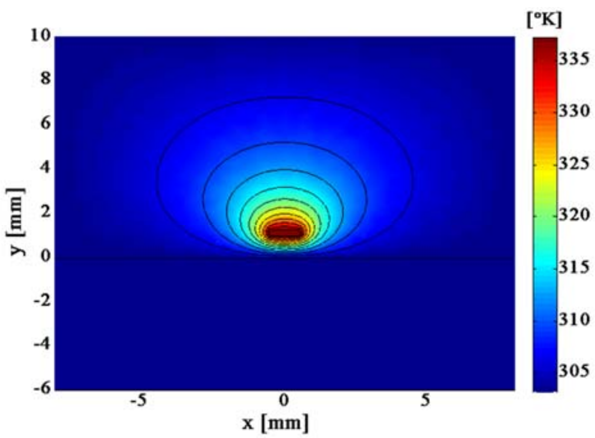

Fig. 10. Temperature distribution computed at steady state for θ=1 and ε=1E-2. Max. Temp.: 337.16 °K, Min. Temp.: 303.15 °K.

VII. CONCLUSION

The BDF-Theta algorithm for the variable time step and order has been applied for the first time to solve a weakly coupled electro-thermal formulation using 2-D first-order finite elements. The electrical power losses due to the Eddy currents and the voltage sources were computed and used in the heat equation. An electrical circuit coupled to thick conductors has been included in the model. A minimum and absolute time step criteria were proposed to incorporate the time steps restrictions from the EDE and the HE. The proposed time-step criterion avoids small time steps and model instabilities. The developed model was programmed in C language and used to solve a numerical example.

ACKNOWLEDGMENT

The authors would like to thank to CONACYT, PROMEP, DGEST, and Instituto Tecnológico de la Laguna for their financial support.

REFERENCES

[1] M. Celuch, M. Soltysiak, and U. Erle, "Computer simulations of microwave heating with coupled electromagnetic, thermal, and kinetic phenomena," *ACES Journal*, vol. 26, no. 4, pp. 275-283, April 2011.

[2] G. Henneberger, K. Sattler, and W. Hadrys, "Coupling of magnetic and fluid flow problems and its application in induction melting apparatus," *IEEE Trans. On Magn.*, vol. 29, no. 2, pp. 1589-1594, 1993.

[3] K. Preis, O. Biro, G. Buchgraber, and I. Ticar, "Thermal-electromagnetic coupling in the finite element simulation of power transformers," *IEEE Trans. On Magn.*, vol. 42, no. 4, pp. 999-102, 2006.

[4] C. Rosas, N. Moraga, V. Bubnovich, and R. Fisher, "Improvement of the cooling process of oil-immersed electrical transformers using heat pipes," *IEEE Trans. On Magn.*, vol. 20, no. 3, pp. 1955-1961, 2005.

[5] V. M. Kulkarni, K. N. Seetharamu, P. A. Aswatha Narayana, A. I. Azid, and G. A. Quadir, "Flow analysis for flip chip underfilling process using characteristic based split method," *IEEE Electronics Packaging Technology Conf.*, pp. 615-619, Feb. 2004.

[6] M. Sadiku, "A simple introduction to finite element analysis of electromagnetic problems," *IEEE Trans. On Education*, vol. 32, no. 2, pp. 85-93, 1989.

[7] J. H. Alwash and L. J. Qaseer, "Three-dimension finite element analysis of a helical motion induction motor," *ACES Journal*, vol. 25, no. 8, pp. 703-712, August 2010.

[8] I. A. Tsukerman, A. Konrad, G. Bedrosian, and M. V. K. Chari, "A survey of numerical methods for transient Eddy current problems," *IEEE Trans. On Magn.*, vol. 29, no. 2, pp. 1711-1716, Mar. 1993.

[9] Q. Wang, C. Yan, Y. Shi, D. Ding, and R. Chen, "Transient analysis of electromagnetic scattering using marching-on-in-order time-domain integral equation method with curvilinear RWG basis functions," *ACES Journal*, vol. 26, no. 5, pp. 429-436, May 2011.

[10] K. E. Brenan, S. L. Campbell, and L. R. Petzold, *Numerical Solution of Initial Value Problems in Differential-Algebraic Equations*, Society for

Industrial and Applied Mathematics, pp. 41-148, 1996.

[11] R. K. Brayton, F. G. Gustavson, and G. D. Hachtel, "A new efficient algorithm for solving differential algebraic systems using implicit backward differentiation formulas," *Proceedings of the IEEE*, vol. 60, no. 1, pp. 98-108, January 1972.

[12] G. J. Barclay, D. F. Griffiths, and D. J. Higham, "Theta method dynamics," *LMS Journal of Computation and Mathematics*, vol. 3, pp. 27-43, Feb. 2000.

[13] O. C. Zienkiewics and R. L. Taylor, *The Finite Element Method Vol. 3 Fluid Dynamics*, Butterworth Heinemann, pp. 64-90, 2000.

[14] R. B. B. Ovando-Martinez, M. A. Arjona Lopez, and C. Hernandez Flores, "A finite-element variable time-stepping algorithm for solving the electromagnetic diffusion equation," *IEEE Trans. On Magn.*, vol. 48, no. 2, pp. 647-650, 2012.

[15] J. Jin, W. Quan-di, Y. Ji-hui, and Z. Ya-li, "Wideband equivalent circuit model and parameter computation of automotive ignition coil based on finite element analysis," *ACES Journal*, vol. 25, no. 7, pp. 612-619, July 2010.

[16] M. A. Arjona, R. B. B. Ovando-Martinez, and C. Hernandez, "Thermal-fluid transient two-dimensional characteristic-based-split finite-element model of a distribution transformer," *IET Electr. Power Appl.*, vol. 6, no. 5, pp. 260-267, 2012.

[17] M. A. Taghikhani and A. Gholami, "Heat transfer in power transformer windings with oil-forced cooling," *IET Electr. Power Appl.*, vol. 3, no. 1, pp. 59-66, 2009.

[18] J. P. A. Bastos and N. Sadowski, *Electromagnetic Modeling by Finite Element Methods*, Marcel-Dekker, 2003.

[19] T. Boonen, J. Van Lent, H. De Gersem, J. Driesen, and S. Vandewalle, "Algebraic multigrid for implicit Runge-Kutta discretizations of the Eddy current problem," *IEEE Trans. On Magn.*, vol. 43, no. 4, pp. 1265-1268, April 2007.

[20] A. Nicolet and F. Delincé, "Implicit Runge-Kutta methods for transient magnetic field computation," *IEEE Trans. On Magn.*, vol. 32, no. 3, pp. 1405-1408, May 1996.

[21] L. O. Chua and P. Min, *Computer Aided Analysis of Electronic Circuits algorithms and Computational Techniques*, Prentice Hall, pp. 665-685, 1975.

[22] O. Shenk and K. Gartner, "Solving unsymmetric sparse systems of linear equations with pardiso," *Journal of Future Generation Computer Systems*, vol. 20, no. 3, pp. 475-487, 2004.

[23] O. Shenk and K. Gartner, "On fast factorization pivoting methods for symmetric indefinite systems," *Elec. Trans. On Numberical Analysis*, vol. 23, pp. 158-179, 2006.

[24] R. W. Lewis, P. Nithiarasu, and N. S. Kankanhally, *Fundaments of the Finite Element Method for Heat and Fluid Flow*, Wiley, 2004.

[25] COMSOL Multiphysics user's guide, version 3.5a, COMSOL AB, November 2008.

R.B.B. Ovando-Martinez received the B.Sc. degree in Electrical Engineering from the Instituto Tecnológico de la Laguna, Torreón, México, in 2008, the M.Sc. degree in Electrical Engineering from the Instituto Tecnológico de la Laguna, Torreón, México, in 2009. He is currently working toward his Sc.D. degree in Electrical Engineering at the Instituto Tecnológico de la Laguna. His research interest includes electromagnetic, thermal and fluid dynamics modeling of electrical machines.

C. Hernandez received the B.Sc. degree in Computer Science from the Instituto Tecnológico de Estudios Superiores de Monterrey, Monterrey, México, in 1990, the M.Sc. degree in foundations of advanced information technology from Imperial College, London, U.K., in 1995, and the Sc.D. degree in Electrical Engineering from the Instituto Tecnológico de la Laguna, Torreón, México, in 2007. She was with the Simulation Department, Instituto de Investigaciones Eléctricas from 1991 to 2000. She is currently with the Instituto Tecnológico de la Laguna, Torreón, México. Her interests are in artificial intelligence and global optimization applied to electrical machines.

M. A. Arjona received the B.Sc. degree in Electrical Engineering from the Instituto Tecnológico de Durango, Durango, México, in 1988, the M.Sc. degree in Electrical Engineering from the Instituto Tecnológico de la Laguna, Torreón, México, in 1990, and the Ph.D. degree in Electrical Engineering from Imperial College, London, U.K., in 1996. He was with the Simulation Department, Instituto de Investigaciones Eléctricas from 1991 to 1999. He is currently a Professor of electrical machines with the Instituto Tecnológico de la Laguna. His interests are in the electromagnetic design, analysis, and control of electrical machines.